Electronic Supplementary Material (ESI) for Journal of Materials Chemistry A.

Electronic Supplementary Information

The role of uniformly distributed ZnO nanoparticles on cellulose nanofiber for flexible solid state symmetric supercapacitors

Iqra Rabani[a], Jeseung Yoo[a], Chinna Bathula[b], Sajjad Hussain[a] and Young-Soo Seo[a*]

[a]Department of Nanotechnology and Advanced Materials Engineering, Sejong University, Seoul 05006, Republic of Korea.

[b]Division of Electronics and Electrical Engineering, Dongguk University-Seoul, Seoul 04620, Republic of Korea

*****Corresponding author E-mail: ysseo@sejong.ac.kr

Figure Captions

Figure S1. Schematic illustration of the 1D-CNF@ZnO paper based FSS-SC device.

Figure S2. Galvanostatic charging-discharging (GCD) curve of 1D-CNF@ZnO-1 hybrid in a three electrode configuration.

Figure S3. GCD curve of 1D-CNF@ZnO-2 hybrid in a three electrode configuration.

Figure S4. GCD curve of 1D-CNF@ZnO-3 hybrid in a three electrode configuration.

Figure S5. GCD curve of 1D-CNF@ZnO-4 hybrid in a three electrode configuration.

Figure S6. Cyclic voltammetry (CV) of the pristine ZnO NPs in a three electrode configuration.

Figure S7. CV curve of the 1D-CNF in a three electrode configuration.

Figure S8. CV curve of the pristine ZnO NPs in a three electrode configuration.

Figure S9. CV curve of the 1D-CNF in a three electrode configuration.

Figure S10. CV curve of the solid state symmetric device of the pristine ZnO NPs.

Figure S11. CV curve of the solid state symmetric device of the 1D-CNF.

Figure S12. GCD curve of the solid state symmetric device of the pristine ZnO NPs.

Figure S13. GCD curve of the solid state symmetric device of the 1D-CNF.

Figure S14. Coulombic efficiency (%) of the 1D-CNF@ZnO hybrid solid state symmetric supercapacitor device.

Figure S15. Photo digital images of the 1D-CNF@ZnO paper before and after calcinations.

Figure S16. CV curves of 1D-CNF@ZnO at different thickness of the paper such as **(a)** 0.123 mm, **(b)** 0.098 mm and **(c)** 0.072 mm and **(d)** 0.056 mm, respectively.

Figure S17. GCD curves of 1D-CNF@ZnO at different thickness of the paper such as **(a)** 0.123 mm, **(b)** 0.098 mm and **(c)** 0.072 mm, respectively.

Figure S18. CV and GCD curves of 1D-CNF@ZnO with the 0.0156 mm thickness of the paper such as **(a)** comparison CV curve at 10 mVs^{-1} before and after stability, **(b)** comparison GCD curve at 1 A/g of current density before and after stability test.

Figure S19. FESEM micrographs of the 1D-CNF@ZnO paper after stability test.

Table S1. Comparative electrochemical performance of 1D-CNF@ZnO in the three-electrode system with other previously reported materials.

Table S2. Comparative electrochemical performance of 1D-CNF@ZnO in all solid state symmetric/Asymmetric supercapacitor devices with other previously reported materials.

References

1.1 Structural characterization detail

The interior structural properties characterized morphology and chemical composition of the 1D-CNF@ZnO hybrid were investigated using the TESCAN Mira3 field-emission scanning electron microscope (FESEM) accompanying with energy dispersive X-ray (EDX). Transmission electron microscopy (TEM) and high-resolution transmission electron microscopy were analyzed by the JEM 2010 FEF (UHR) microscope (JEOL) at 400 keV. The as prepared sample was dispersed into the absolute ethanol solution and then ultrasonication for a while. The 1μL drop was added into the carbon grid and then dried into the vacuum oven The structural measurement was further examined using the X-ray diffractogram (XRD, Panalytical). The spectra of Cu Kα, λ= 0.15418 nm at the 30 mA and 40 kV were recorded in the 2θ region from 10 to 80 at a scanning speed of the 2°/min. X-ray photoelectron spectroscopy (XPS) were characterized by an ESCALAB 250Xi (Thermo Scientific) X-ray photoelectron spectrometer with monochromatic Al Kα (1486.6 eV) radiation as the excitation source. The Brunauer−Emmett−Teller (BET) surface area and Barret−Joyner−Halenda (BJH) pore analysis were done using a Quantachrome NOVA 2000e sorption analyzer at liquid nitrogen temperature (77 K).

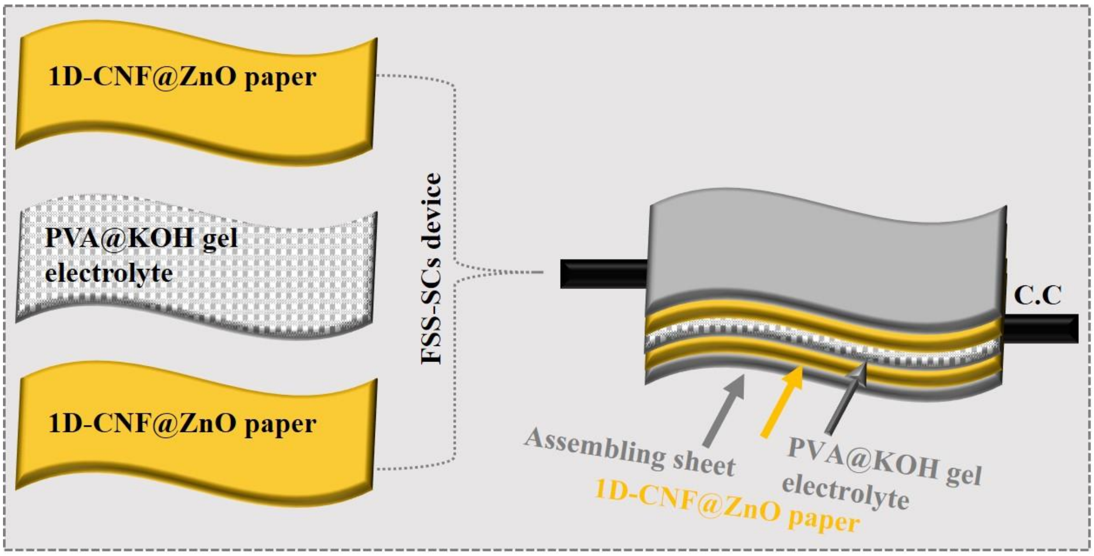

Figure S1. Schematic illustration of the 1D-CNF@ZnO paper based FSS-SC device.

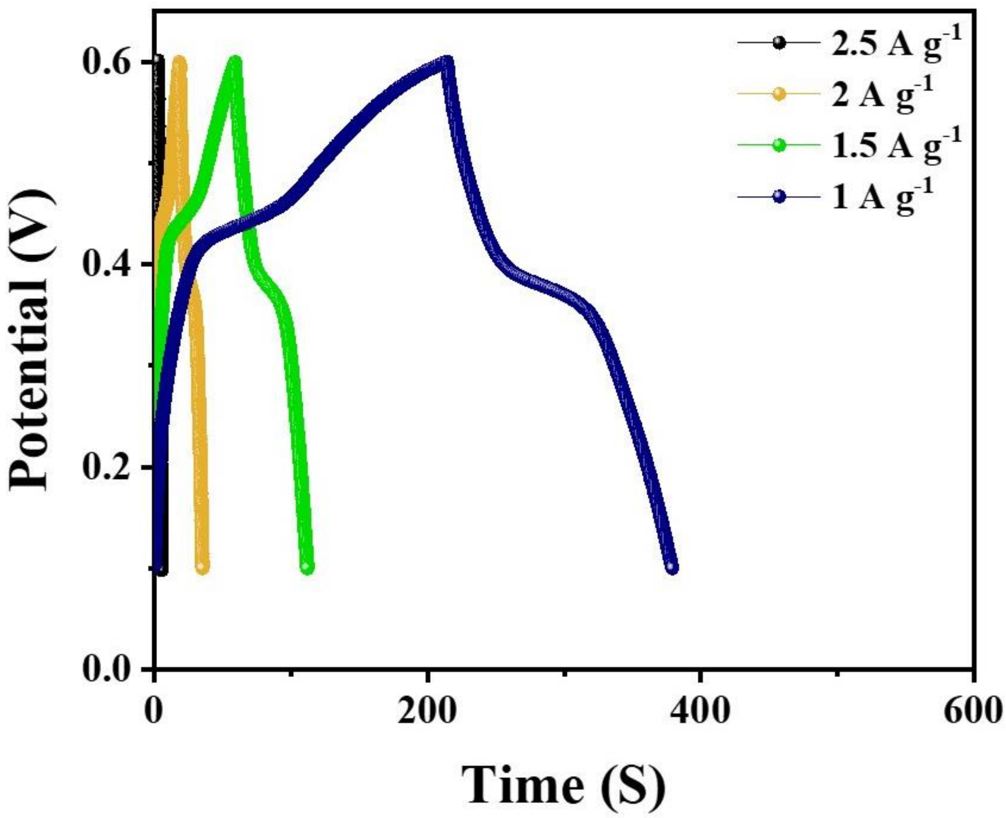

Figure S2. Galvanostatic charging-discharging (GCD) curve of 1D-CNF@ZnO-1 hybrid in a three electrode configuration.

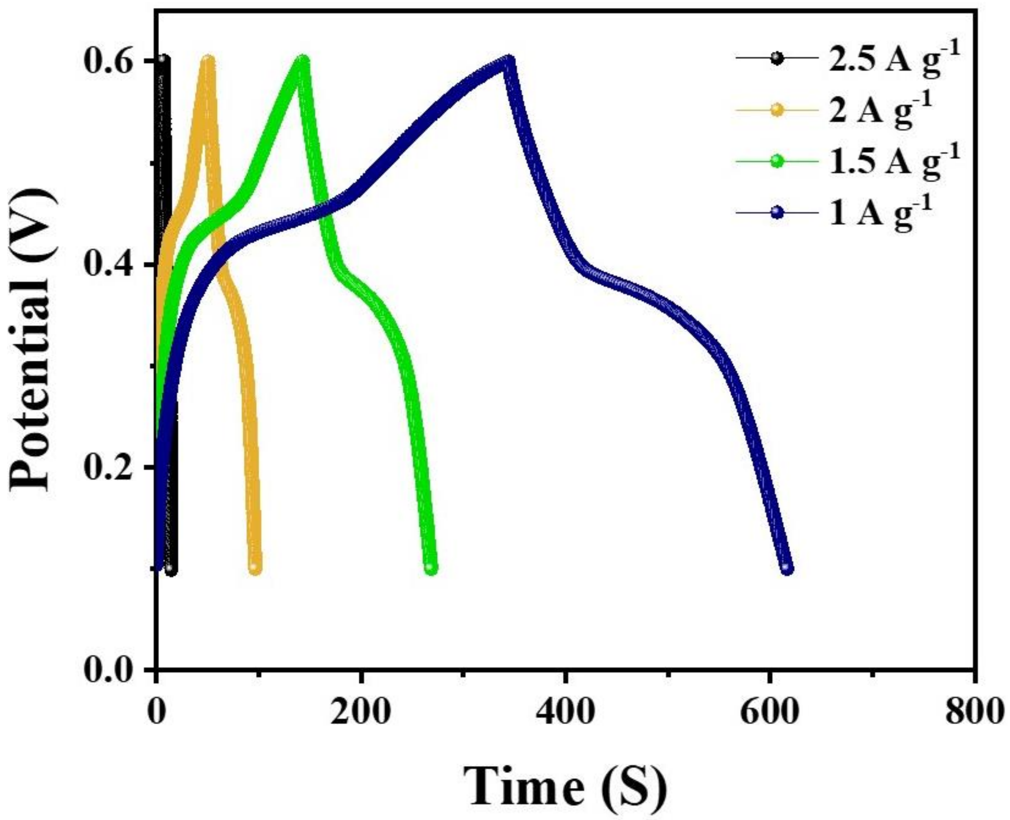

Figure S3. GCD curve of 1D-CNF@ZnO-2 hybrid in a three electrode configuration.

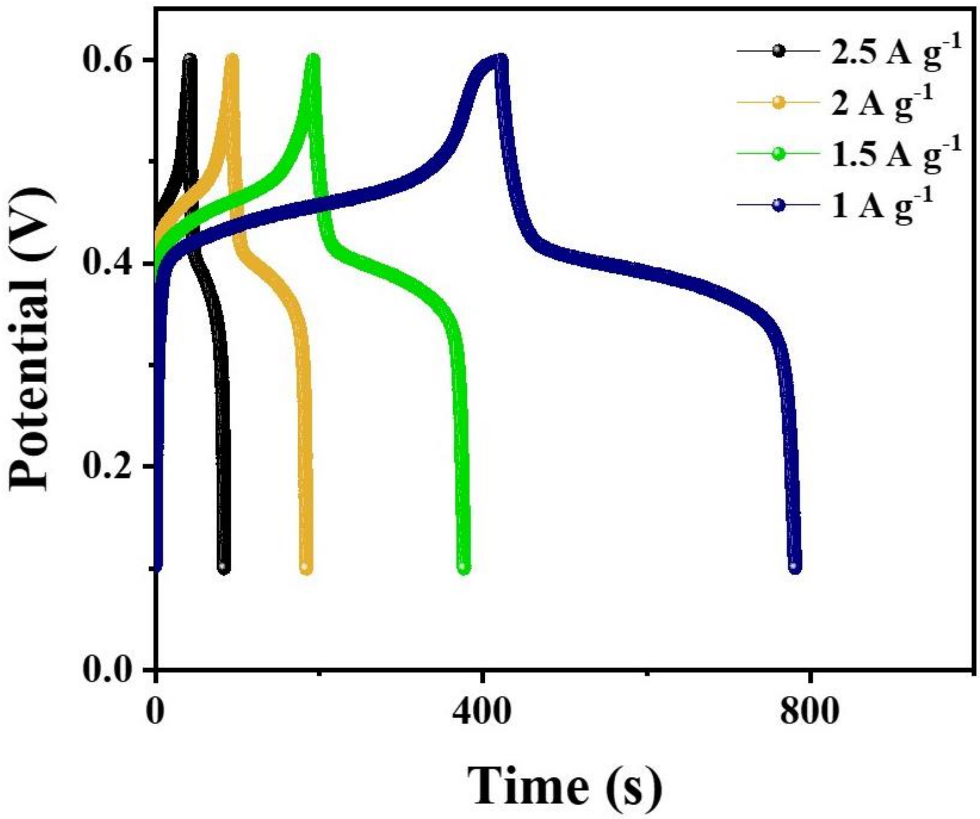

Figure S4. GCD curve of 1D-CNF@ZnO-3 hybrid in a three electrode configuration.

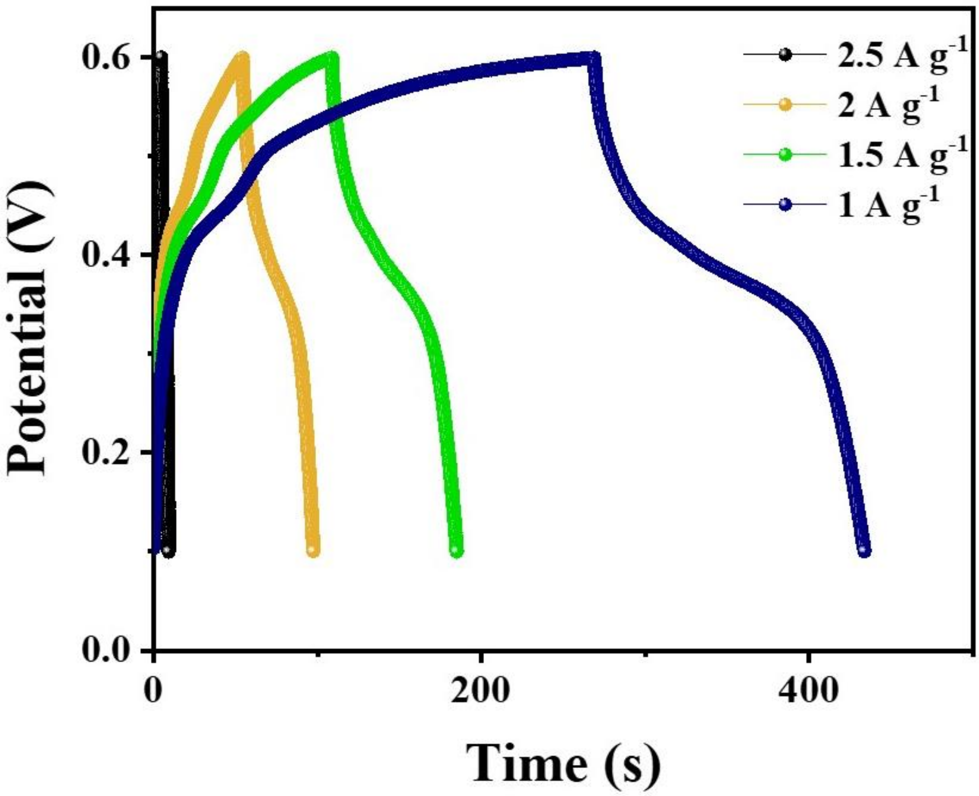

Figure S5. GCD curve of 1D-CNF@ZnO-4 hybrid in a three electrode configuration.

.

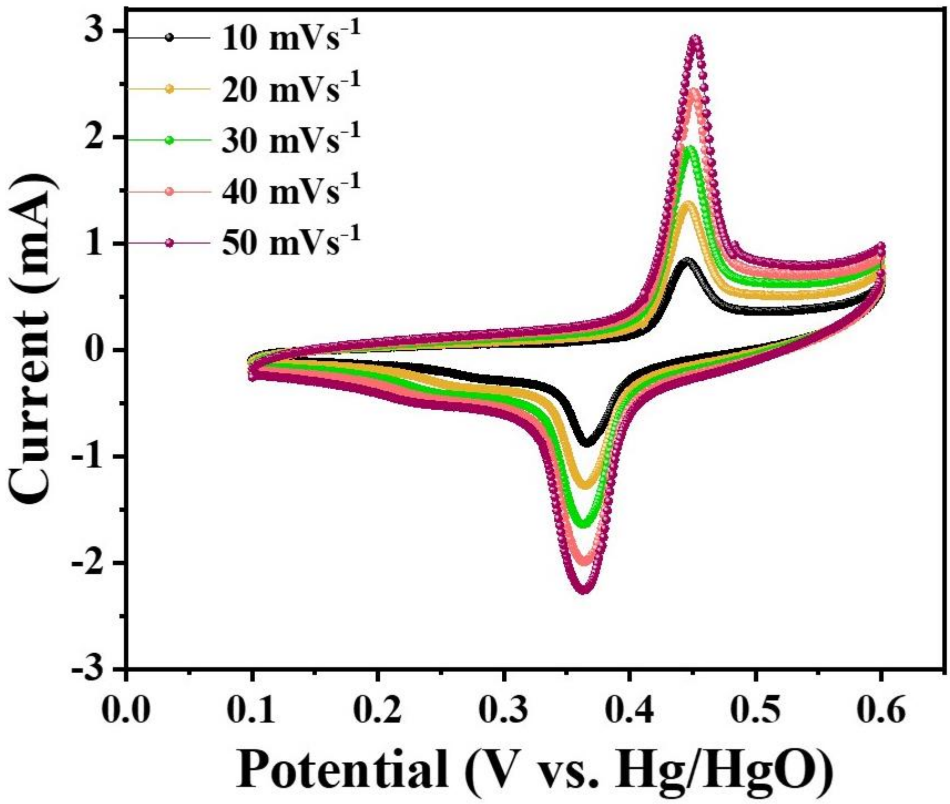

Figure S6. Cyclic voltammetry (CV) of the pristine ZnO NPs in a three electrode configuration.

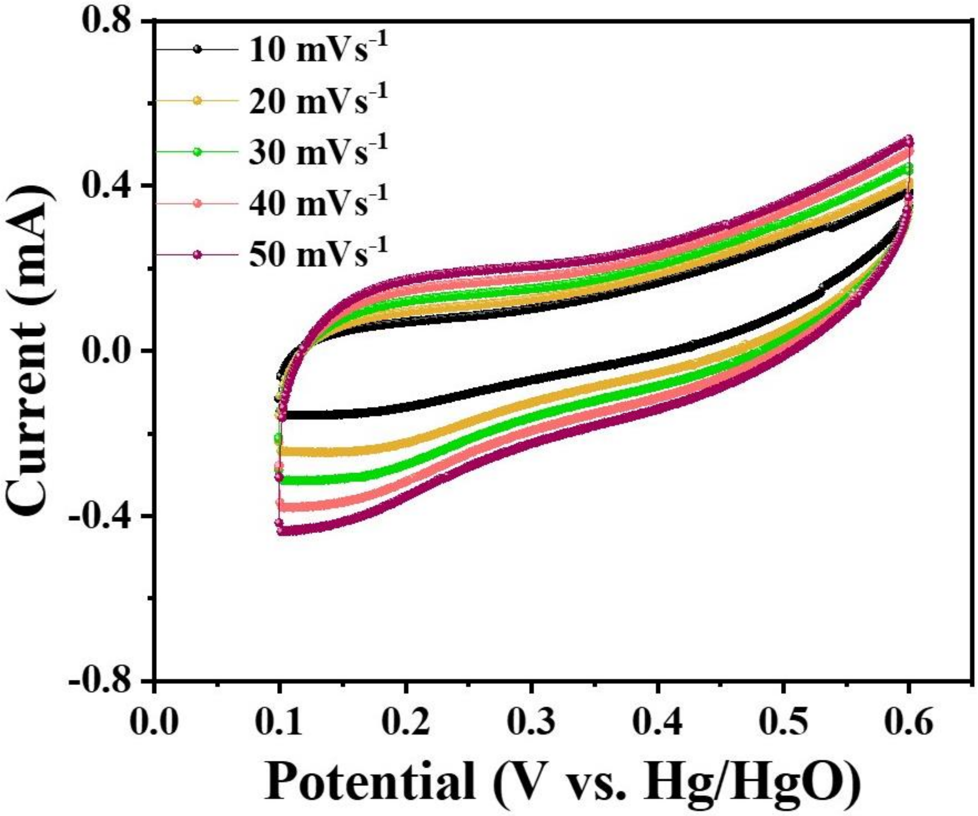

Figure S7. CV curve of the 1D-CNF in a three electrode configuration.

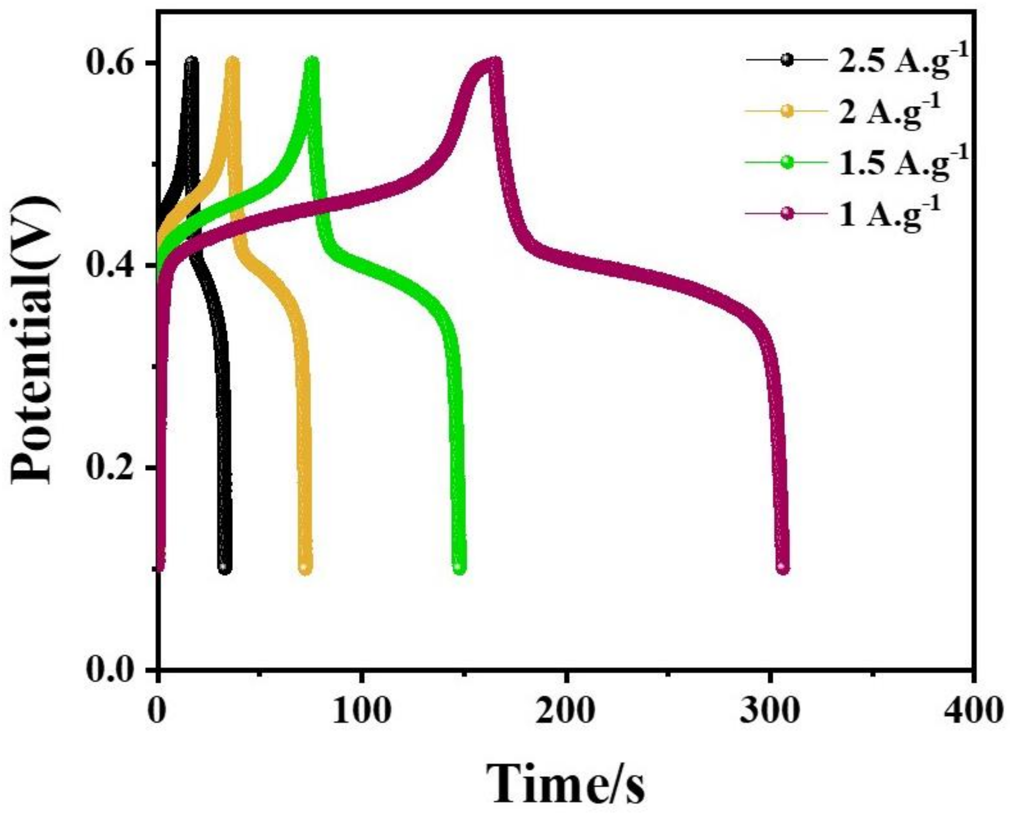

Figure S8. CV curve of the pristine ZnO NPs in a three electrode configuration.

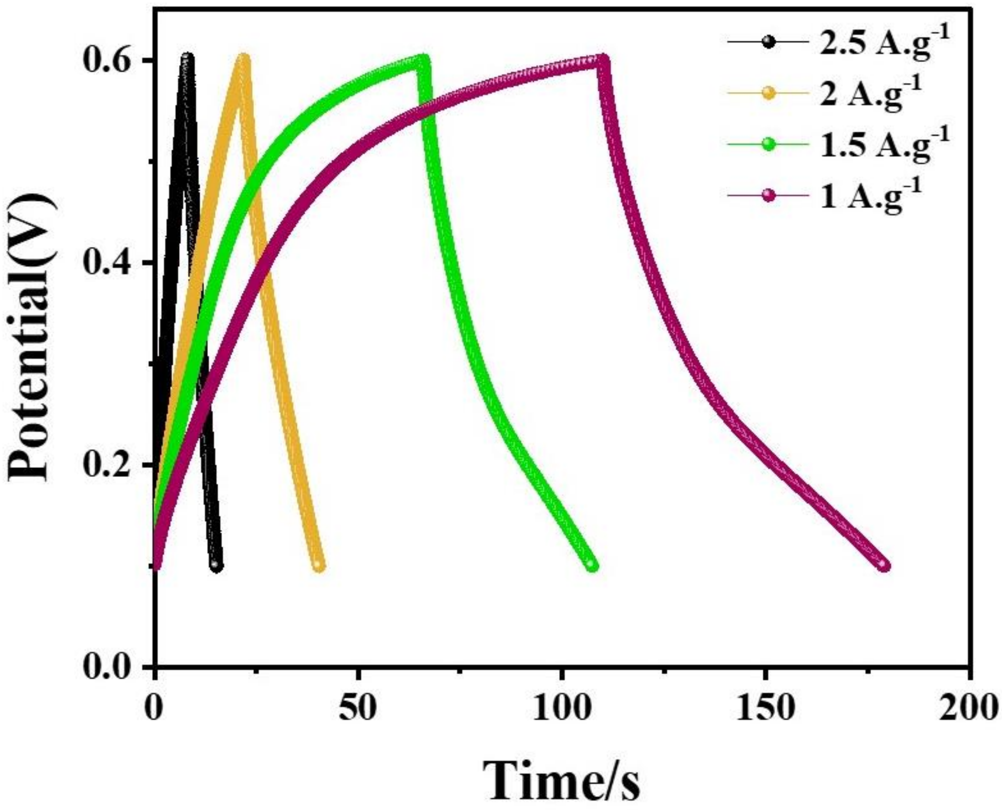

Figure S9. CV curve of the 1D-CNF in a three electrode configuration.

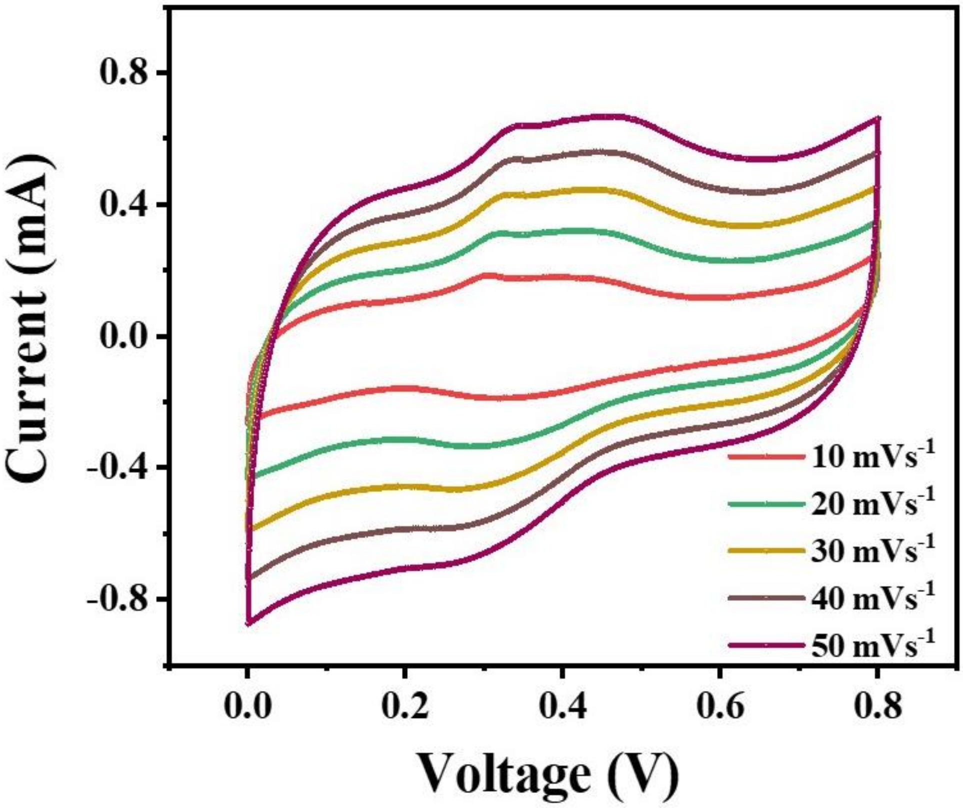

Figure S10. CV curve of the solid state symmetric device of the pristine ZnO NPs.

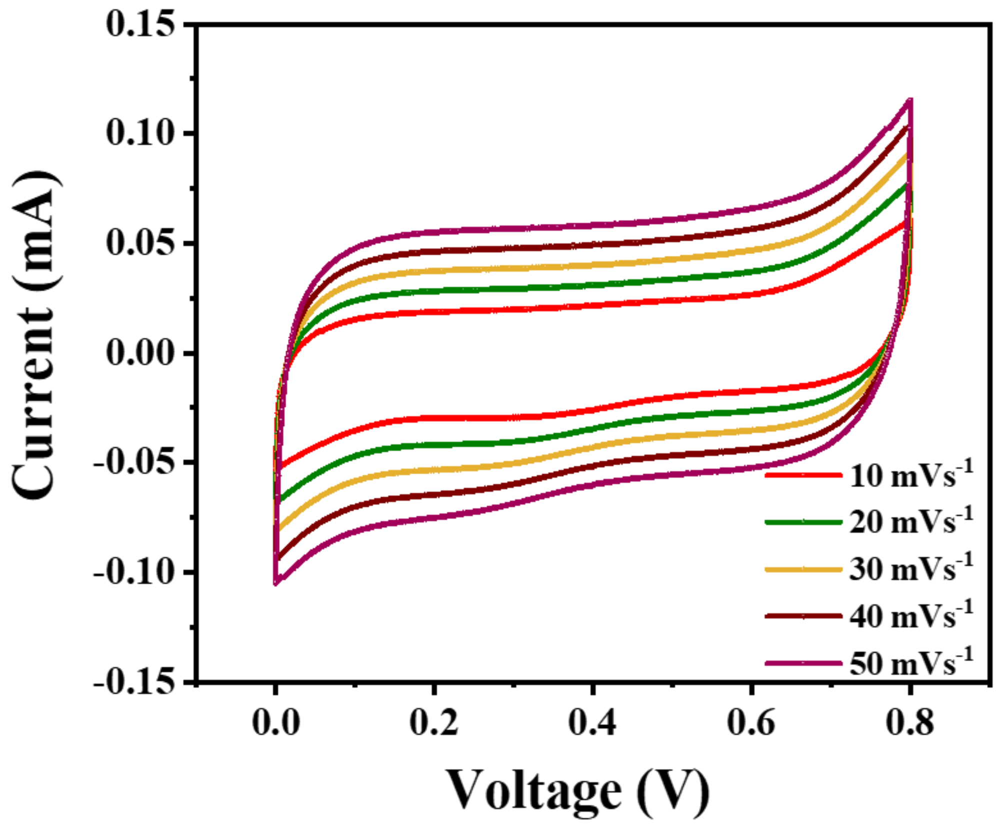

Figure S11. CV curve of the solid state symmetric device of the 1D-CNF.

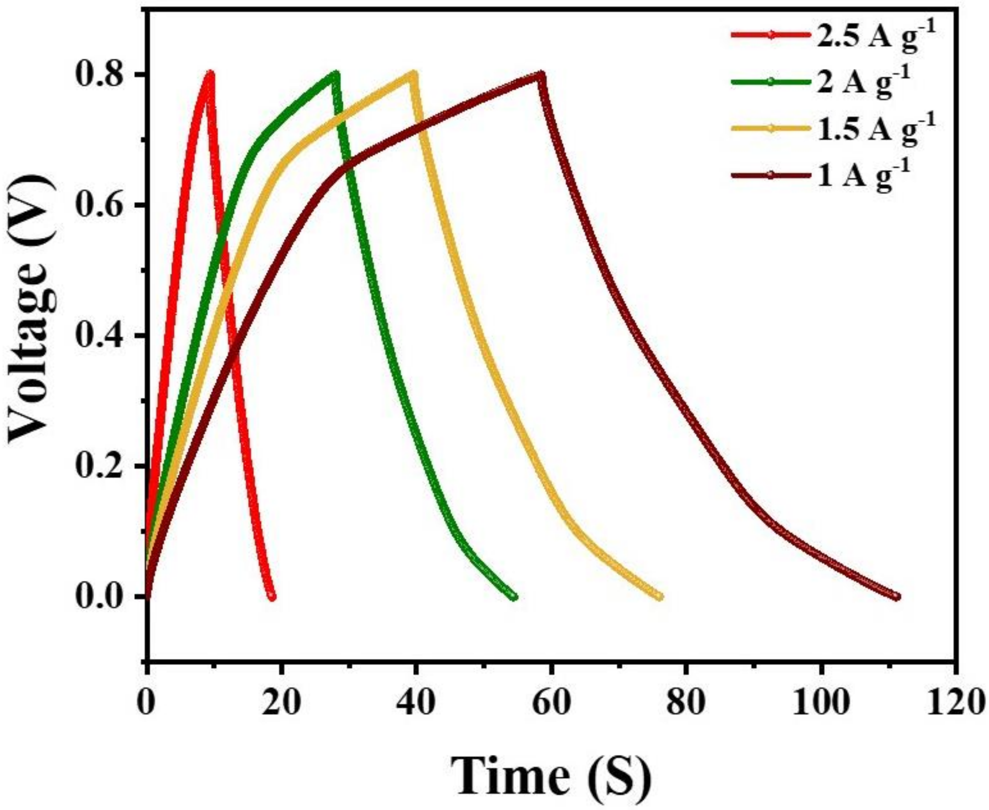

Figure S12. GCD curve of the solid state symmetric device of the pristine ZnO NPs.

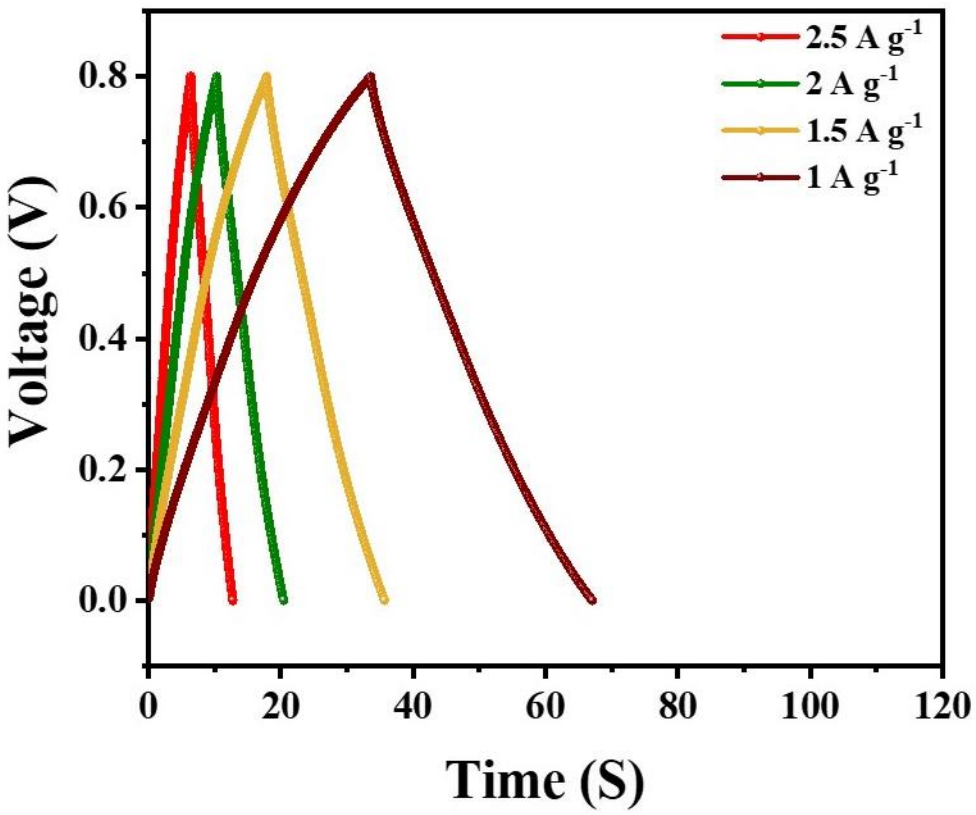

Figure S13. GCD curve of the solid state symmetric device of the 1D-CNF.

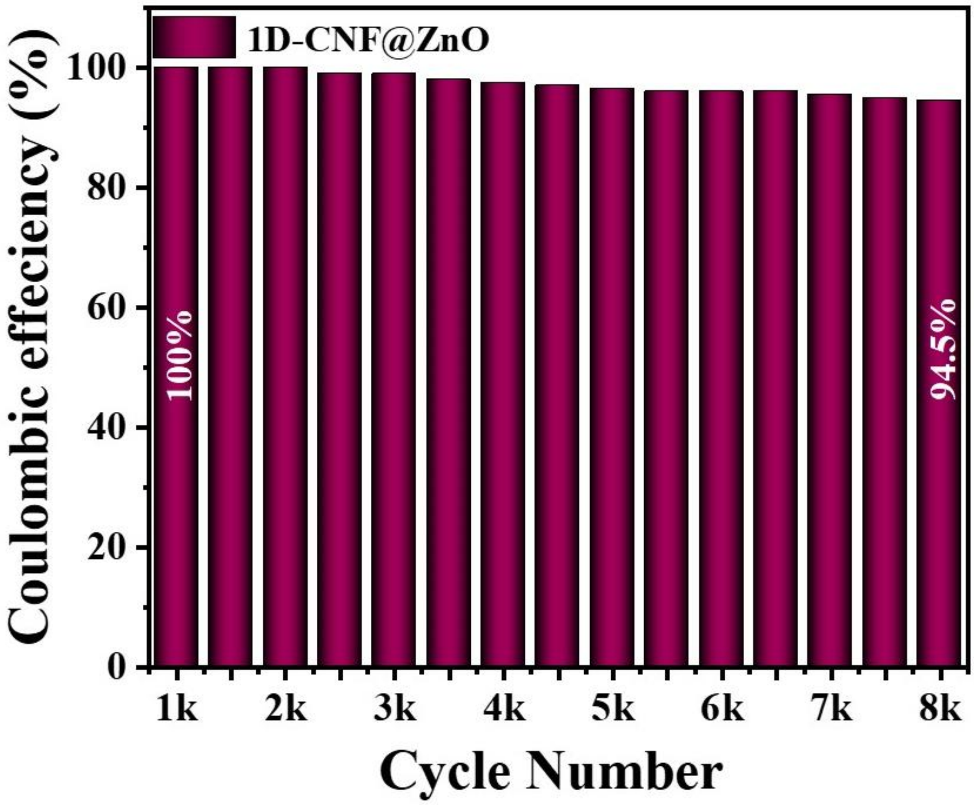

Figure S14. Coulombic efficiency (%) of the 1D-CNF@ZnO hybrid solid state symmetric supercapacitor device.

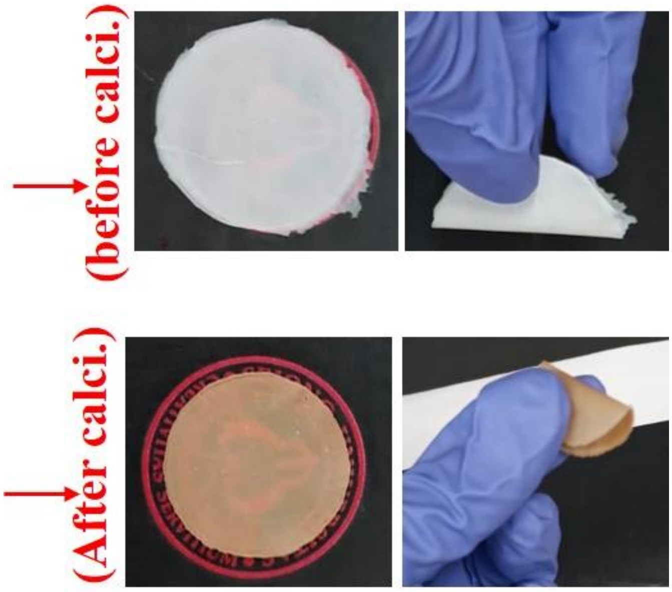

Figure S15. Photo digital images of the 1D-CNF@ZnO paper before and after calcinations.

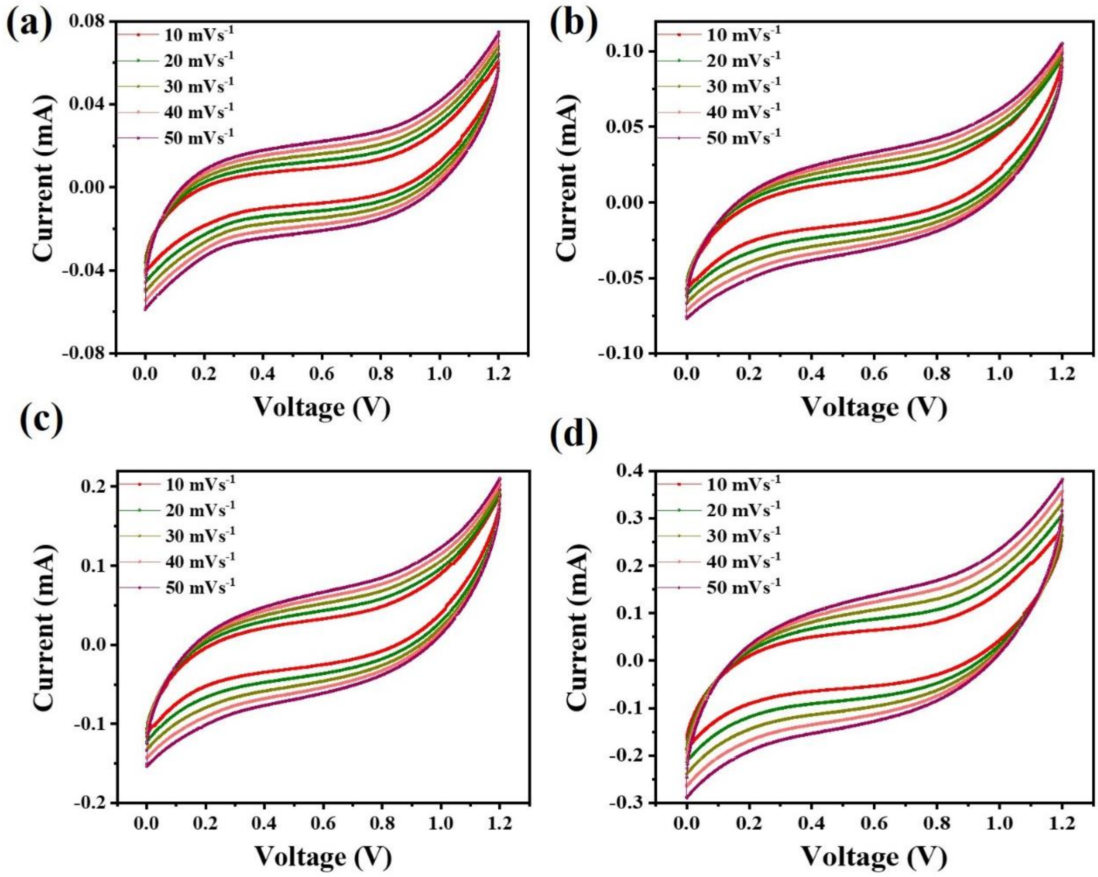

Figure S16. CV curves of 1D-CNF@ZnO paper FSS-SC devices at different thickness of the paper such as **(a)** 0.123 mm, **(b)** 0.098 mm, **(c)** 0.072 mm and **(d)** 0.056 mm, respectively.

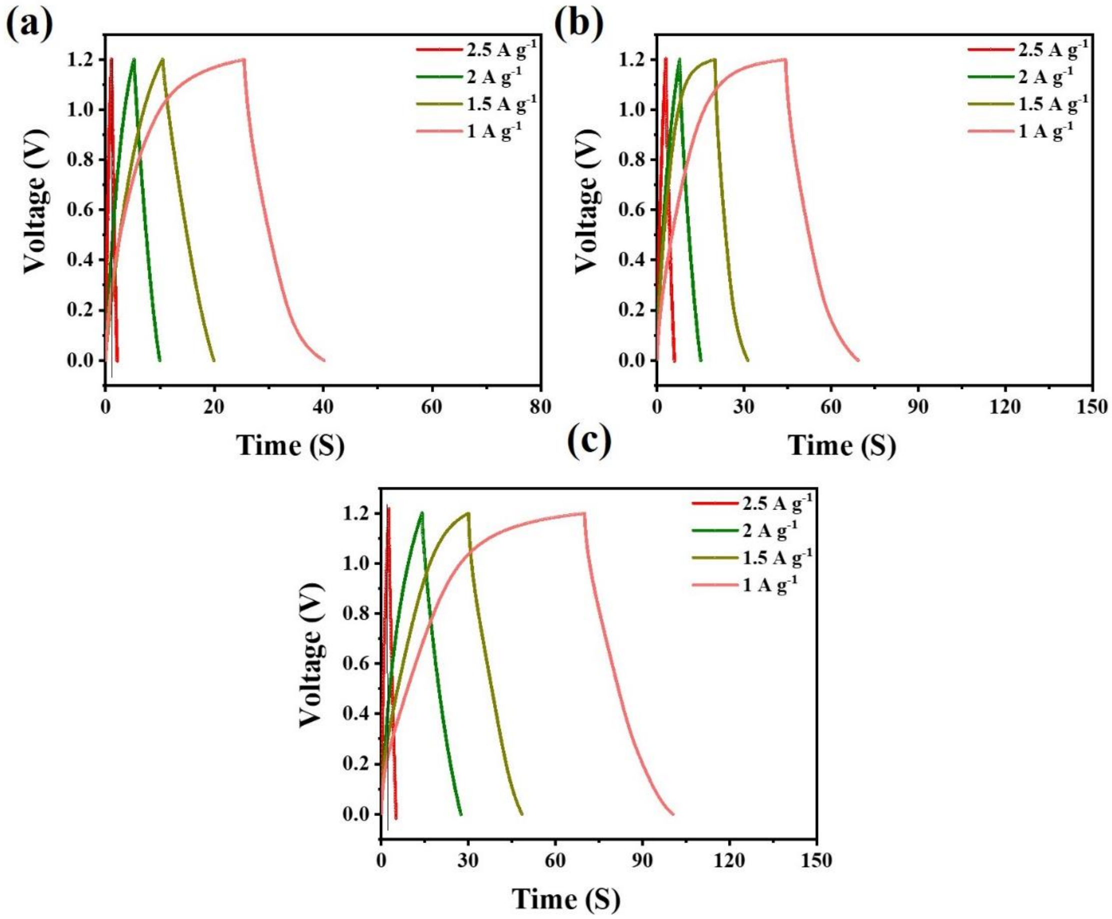

Figure S17. GCD curves of 1D-CNF@ZnO at different thickness of the paper such as **(a)** 0.123 mm, **(b)** 0.098 mm and **(c)** 0.072 mm, respectively.

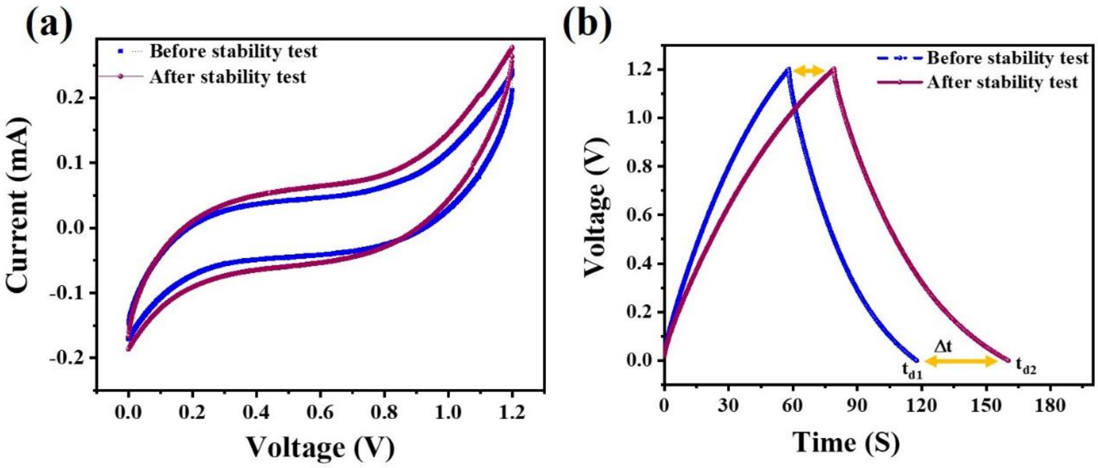

Figure S18. CV and GCD curves of 1D-CNF@ZnO with the 0.0156 mm thickness of the paper such as **(a)** comparison CV curve at 10 mVs^{-1} before and after stability, **(b)** comparison GCD curve at 1 A/g of current density before and after stability test.

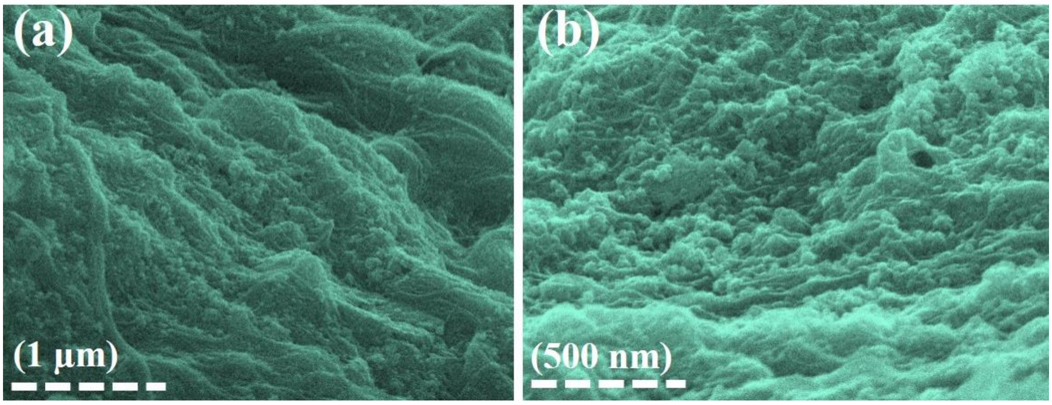

Figure S19. FESEM micrographs of the 1D-CNF@ZnO paper after stability test.

Table S1. Comparative electrochemical performance of 1D-CNF@ZnO in the three-electrode system with other previously reported materials.

Electrode materials	Electrolyte	Voltage window	Specific capacitance	Ref.
1D-CNF@ZnO	**6 M KOH**	**0.1 to 0.6**	**748 $F.g^{-1}$ at 1 $A{\cdot}g^{-1}$**	**Present work**
CC/ZnO@C@NiO	3 M KOH	0 to 0.8 V	677 $F.g^{-1}$ at 1.4 $A{\cdot}g^{-1}$	1
ZnO-NiO composite			643 $F.g^{-1}$ at 5.8 $A{\cdot}g^{-1}$	2
NiO/ultrathin graphene			425 $F.g^{-1}$ at 2 $A{\cdot}g^{-1}$	3
ZnO/MnO_2 Urchin	0.5 M Na_2SO_4	0 to 0.8	262 $F.g^{-1}$ at 0.2 $A{\cdot}g^{-1}$	4
$ZnMn_2O_4/C$	6 M KOH	0 to 1.2 V	589 $F.g^{-1}$ at 1 $A{\cdot}g^{-1}$	5
ZnO/MnO	1 M Na_2SO_4	0 to 0.8	14 mF/cm^2 at 0.1 mA/cm^2	6
ZnO/MnO_2 nanowires	1 M Na_2SO_4	0 to 0.9	501 $F.g^{-1}$ at 2 $A{\cdot}g^{-1}$	7
$ZnMn_2O_4$/carbon	6 M KOH	-1 to -0.3	105 $F.g^{-1}$ at 0.3 $A{\cdot}g^{-1}$	8
ZnO nanocones	1 M KOH	0.1 to 0.6	236 $F.g^{-1}$ at 1 $A{\cdot}g^{-1}$	9
NCA/Co_3O_4	6 M KOH	-0.05 to 0.45 V	616 $F{\cdot}g^{-1}$ at 1.2 $A{\cdot}g^{-1}$	10
$CuCo_2S_4$/CNT/graphene	1 M Na_2SO_4	0 to 0.6 V	504 $F{\cdot}g^{-1}$ at 10 $A{\cdot}g^{-1}$	11
CPSC-3rGO	0.2 M Na_2SO_4	-0.2 to 0.8 V	446 $F{\cdot}g^{-1}$ at 1 $A{\cdot}g^{-1}$	12
CS@ZnO Core-shell	6 M KOH	0 to 0.4	630 $F{\cdot}g^{-1}$ at 2 $A{\cdot}g^{-1}$	13
3D graphene ZnO nanorods	1 M KOH		554.23 $F{\cdot}g^{-1}$ at 5 mV/s	14
ZnO/carbon	6 M KOH		500 $F{\cdot}g^{-1}$ at 100 mV/s	15
Co_3O_4 nanoflakes@SrGO	2 M KOH	-0.2 to 0.5 V	406 $F{\cdot}g^{-1}$ at 1 $A{\cdot}g^{-1}$	16
$CoMoO_4$ nanoclusters	6.0 M KNO_3	−0.9 to 0.6 V	367 $F{\cdot}g^{-1}$ at 1.2 $A{\cdot}g^{-1}$	17
Ni-Co selenide	6 M KOH	0 to 0.6 V	742.4 $F{\cdot}g^{-1}$ at 1 $mA\ cm^{-2}$	18
$NiCo_2O_4$	6 M KOH	-0.2 to 0.6 V	225 C. g^{-1} at 0.5 A g^{-1}	19

Table S2. Comparative electrochemical performance of 1D-CNF@ZnO in all solid state symmetric/Asymmetric supercapacitor devices with other previously reported materials.

Electrode materials	Type	Electrolyte	Specific capacitance	Capacitance retention (%)/cycles	Ref.
1D-CNF@ZnO	**Symmetric**	**PVA-KOH gel**	**220 $F \cdot g^{-1}$ @ 1.0 $A \cdot g^{-1}$**	**88/8000**	**Present**
CoNW/CF//CoNW/CF SSC	Symmetric	3.0 M KOH	517.33 mF/cm^3 @ 0.26 mA/cm^2	95/5000	20
NCOs	Symmetric	1.0 M KOH	89 F g^{-1} @ 0.23 $A.g^{-1}$	-	21
CNF-RGO	Symmetric	H_2SO4-PVA	203 F g^{-1} @ 0.7 mA/cm^2	99/5000	22
1D-$CoSe_2$ nanoarrays	Symmetric	PVA-KOH	152 F/g @ 0.5 A/g	96.8/5000	
ZnO/Co_3O_4-450//AC	Asymmetric	1.0 M KOH	153 F g^{-1} @ 1 $A.g^{-1}$	-	23
$CC@NiC_2O_4$ //CC@NC	Asymmetric	6.0 M KOH	89.7 F g^{-1} @ 1 A g^{-1}	86.7/20000	24
$Co_3O_4@Ni_3S_2$	Asymmetric	3.0 M KOH	126 F g^{-1} @ 1 $A.g^{-1}$	83.5/5000	25
Ag/NiO	Asymmetric	3.0 M KOH	204 $C.g^{-1}$ @ 2.5 $A.g^{-1}$	96/4000	26
Co_3O_4@Ni(OH)2//AC	Asymmetric	6.0 M KOH	110 $F.g^{-1}$ @ 2.5 $A.g^{-1}$	86/1000	27
3D graphene-MoS_2 hybrid	Symmetric	KOH/PVA	58.0$F.g^{-1}$@ 2 $A.g^{-1}$	-	28
TaS_2	Symmetric	PVA/LiCl	508 F/cm^3 @ 10 mV/s	92/4000	29
Cu_2WS_4	Symmetric	PVA/LiCl	583.3 F cm^{-3} @ 0.31 A cm^{-3}	95/3000	30
MoS_2-NH_2/PANI nanosheets	Symmetric	1 M H_2SO_4	58.6 F g^{-1} @ 2 $A.g^{-1}$	96.5/10000	31
MoS_2/CNS	Symmetric	1 M Na_2SO_4	108 F g^{-1} @ 1 $A.g^{-1}$	-	32
MoS_2/G nanobelts	Symmetric	1 M Na_2SO_4	278.2 $F.g^{-1}$ @ 0.8 $A.g^{-1}$	-	33

MoS_2/rGO	Symmetric	1 M H_2SO_4	306 $F.g^{-1}$ @ 0.5 $A.g^{-1}$	-	34
NiS/MoS2@N-rGO	Symmetric	6 M KOH	1028 $F.g^{-1}$ @1 $A.g^{-1}$	94.5/50000	35
VSL-MoS2@3D-Ni foam	Symmetric	Na_2SO_4/PVA	34.1 $F.g^{-1}$@ 1.3 $A.g^{-1}$	82.5/10000	36
MoS_2/rGO	Symmetric	NaOH	323 $F.g^{-1}$ @ 0.2 $A.g^{-1}$	76.8/500	37
SS/MWCNTs/$MoTe_2$	Symmetric	PVA-$LiClO_4$	68.01 $F.g^{-1}$ @ 0.2 $mA.cm^{-2}$	94/2000	38
MWCNTs/$MoSe_2$	Symmetric	PVA-KOH	27 $F.g^{-1}$ @ 0.4 A/g	95/1000	39
MoS_2/carbon cloth	Symmetric	PVA-$LiClO_4$	368 $F.g^{-1}$ @ 5 mV/s	96.5/5000	40
MoS_2/NPG	Symmetric	1 M Na_2SO_4	102.5 F g^{-1} @ 1 A g^{-1}	91.67/5000	41
$(Ni,Co)_{0.85}Se$//porous graphene	Asymmetric	1.0 M KOH	529.3 mF cm^{-2} @ 1A g^{-1}	85/10000	42
MoS_2/PEI-GO	Asymmetric	Na2SO4	42.9 @ 0.5 A g^{-1}	93.1/8000	43
MoS_{2-x}@CNTs/Ni	Asymmetric	1 M Na_2SO_4	153.1F g^{-1} @ 1 A g^{-1}	91/3000	44

References

1. Y. Ouyang, X. Xia, H. Ye, L. Wang, X. Jiao, W. Lei and Q. Hao, *ACS applied materials & interfaces*, 2018, **10**, 3549-3561.
2. H. Pang, Y. Ma, G. Li, J. Chen, J. Zhang, H. Zheng and W. Du, *Dalton transactions*, 2012, **41**, 13284-13291.
3. C. Wu, S. Deng, H. Wang, Y. Sun, J. Liu and H. Yan, *ACS applied materials & interfaces*, 2014, **6**, 1106-1112.
4. W. Li, G. He, J. Shao, Q. Liu, K. Xu, J. Hu and I. P. Parkin, *Electrochimica Acta*, 2015, **186**, 1-6.
5. Z. Zhu, Z. Wang, Z. Yan, R. Zhou, Z. Wang and C. Chen, *Ceramics International*, 2018, **44**, 20163-20169.
6. C. J. Raj, M. Rajesh, R. Manikandan, J. Y. Sim, K. H. Yu, S. Y. Park, J. H. Song and B. C. Kim, *Electrochimica Acta*, 2017, **247**, 949-957.
7. S. Li, J. Wen, X. Mo, H. Long, H. Wang, J. Wang and G. Fang, *Journal of Power Sources*, 2014, **256**, 206-211.
8. C.-K. Sim, S. R. Majid and N. Z. Mahmood, *Journal of Alloys and Compounds*, 2019, **803**, 424-433.
9. X. He, J. E. Yoo, M. H. Lee and J. Bae, *Nanotechnology*, 2017, **28**, 245402.
10. G. Sun, L. Ma, J. Ran, X. Shen and H. Tong, *Journal of Materials Chemistry A*, 2016, **4**, 9542-9554.
11. N. I. Chandrasekaran, H. Muthukumar, A. D. Sekar, A. Pugazhendhi and M. J. J. o. M. L. Manickam, 2018, **266**, 649-657.
12. J. S. Lee, C. Lee, J. Jun, D. H. Shin and J. Jang, *Journal of Materials Chemistry A*, 2014, **2**, 11922-11929.
13. X. Xiao, B. Han, G. Chen, L. Wang and Y. Wang, *Scientific reports*, 2017, **7**, 1-13.

14. X. Li, Z. Wang, Y. Qiu, Q. Pan and P. Hu, *Journal of Alloys and Compounds*, 2015, **620**, 31-37.

15. D. Kalpana, K. Omkumar, S. S. Kumar and N. Renganathan, *Electrochimica Acta*, 2006, **52**, 1309-1315.

16. M. Qorbani, T.-c. Chou, Y.-H. Lee, S. Samireddi, N. Naseri, A. Ganguly, A. Esfandiar, C.-H. Wang, L.-C. Chen and K.-H. Chen, *Journal of Materials Chemistry A*, 2017, **5**, 12569-12577.

17. J. Li, C. Zhao, Y. Yang, C. Li, T. Hollenkamp, N. Burke, Z.-Y. Hu, G. Van Tendeloo and W. Chen, *Journal of Alloys and Compounds*, 2019, **810**, 151841.

18. Y. Wang, W. Zhang, X. Guo, K. Jin, Z. Chen, Y. Liu, L. Yin, L. Li, K. Yin and L. Sun, *ACS applied materials & interfaces*, 2019, **11**, 7946-7953.

19. H. Fu, Y. Liu, L. Chen, Y. Shi, W. Kong, J. Hou, F. Yu, T. Wei, H. Wang and X. Guo, *Electrochimica Acta*, 2019, **296**, 719-729.

20. P. Howli, S. Das, S. Sarkar, M. Samanta, K. Panigrahi, N. S. Das and K. K. Chattopadhyay, *ACS omega*, 2017, **2**, 4216-4226.

21. X. Lu, X. Huang, S. Xie, T. Zhai, C. Wang, P. Zhang, M. Yu, W. Li, C. Liang and Y. Tong, *Journal of Materials Chemistry*, 2012, **22**, 13357-13364.

22. K. Gao, Z. Shao, J. Li, X. Wang, X. Peng, W. Wang and F. Wang, *Journal of Materials Chemistry A*, 2013, **1**, 63-67.

23. M. Gao, W.-K. Wang, Q. Rong, J. Jiang, Y.-J. Zhang and H.-Q. Yu, *ACS applied materials & interfaces*, 2018, **10**, 23163-23173.

24. C. Guan, X. Liu, W. Ren, X. Li, C. Cheng and J. Wang, *Advanced Energy Materials*, 2017, **7**, 1602391.

25. J. Zhang, J. Lin, J. Wu, R. Xu, M. Lai, C. Gong, X. Chen and P. Zhou, *Electrochimica Acta*, 2016, **207**, 87-96.

26. S. Nagamuthu and K.-S. Ryu, *Scientific reports*, 2019, **9**, 1-11.

27. C.-h. Tang, X. Yin and H. Gong, *ACS applied materials & interfaces*, 2013, **5**, 10574-10582.

28. K. Singh, S. Kumar, K. Agarwal, K. Soni, V. R. Gedela and K. Ghosh, *Scientific reports*, 2017, **7**, 1-12.

29. J. Wu, J. Peng, Z. Yu, Y. Zhou, Y. Guo, Z. Li, Y. Lin, K. Ruan, C. Wu and Y. Xie, *Journal of the American Chemical Society*, 2018, **140**, 493-498.

30. X. Hu, W. Shao, X. Hang, X. Zhang, W. Zhu and Y. Xie, *Angewandte Chemie International Edition*, 2016, **55**, 5733-5738.

31. R. Zeng, Z. Li, L. Li, Y. Li, J. Huang, Y. Xiao, K. Yuan and Y. Chen, *ACS Sustainable Chemistry & Engineering*, 2019, **7**, 11540-11549.

32. T. N. Khawula, K. Raju, P. J. Franklyn, I. Sigalas and K. I. Ozoemena, *Journal of Materials Chemistry A*, 2016, **4**, 6411-6425.

33. Y. Jia, H. Wan, L. Chen, H. Zhou and J. Chen, *Journal of Power Sources*, 2017, **354**, 1-9.

34. H. Ji, S. Hu, Z. Jiang, S. Shi, W. Hou and G. Yang, *Electrochimica Acta*, 2019, **299**, 143-151.

35. X. Xu, W. Zhong, X. Zhang, J. Dou, Z. Xiong, Y. Sun, T. Wang and Y. Du, *Journal of colloid and interface science*, 2019, **543**, 147-155.

36. R. K. Mishra, A. K. Kushwaha, S. Kim, S. G. Seo and S. H. Jin, *Current Applied Physics*, 2019, **19**, 1-7.

37. T. Xue, Y. Yang, X.-H. Yan, Z.-L. Zou, F. Han and Z. Yang, *Materials Research Express*, 2019, **6**, 095029.

38. S. S. Karade and B. R. Sankapal, *ACS Sustainable Chemistry & Engineering*, 2018, **6**, 15072-15082.

39. S. S. Karade and B. R. Sankapal, *Journal of Electroanalytical Chemistry*, 2017, **802**, 131-138.

40. M. S. Javed, S. Dai, M. Wang, D. Guo, L. Chen, X. Wang, C. Hu and Y. Xi, *Journal of Power Sources*, 2015, **285**, 63-69.

41. S. Zhao, W. Xu, Z. Yang, X. Zhang and Q. Zhang, *Electrochimica Acta*, 2020, **331**, 135265.

42. C. Xia, Q. Jiang, C. Zhao, P. M. Beaujuge and H. N. Alshareef, *Nano Energy*, 2016, **24**, 78-86.

43. M.-C. Liu, Y. Xu, Y.-X. Hu, Q.-Q. Yang, L.-B. Kong, W.-W. Liu, W.-J. Niu and Y.-L. Chueh, *ACS Applied Materials & Interfaces*, 2018, **10**, 35571-35579.

44. P. Sun, R. Wang, Q. Wang, H. Wang and X. Wang, *Applied Surface Science*, 2019, **475**, 793-802.